

The SiRi Particle-Telescope System

M. Guttormsen* and A. Bürger
Department of Physics, University of Oslo, Norway

T.E. Hansen and N. Lietaer
SINTEF, Department for Microsystems and Nanotechnology, Oslo, Norway

A silicon particle-telescope system for light-ion nuclear reactions is described. In particular, the system is designed to be optimized for level density and γ -ray strength function measurements with the so-called Oslo method. Eight trapezoidal modules are mounted at 5 cm distance from the target, covering 8 forward angles between $\theta = 40$ and 54° . The thin front ΔE detectors ($130\ \mu\text{m}$) are segmented into eight pads, determining the reaction angle θ for the outgoing charged ejectile. Guard rings on the thick back E detectors ($1550\ \mu\text{m}$) guarantee low leakage current at high depletion voltage.

Keywords: Silicon detectors, particle telescope, coincidences

I. INTRODUCTION

The experimental nuclear physics group at the Oslo Cyclotron Laboratory (OCL) has, through the last decades, investigated the excitation energy region between quantum-order and chaos in nuclei. The group has developed the so-called Oslo method [1], which gives the number of energy levels accessible for the nucleus, as well as the γ -ray strength function from these energetic quantum states.

The OCL group has gained international renown and much attention for its discoveries, see e.g. [2, 3] and references therein. The most important results are (i) experimental evidence for breaking of Bardeen-Cooper-Schrieffer (BCS) pairs and the melt down of pair correlations in the nucleus, (ii) measurements of nuclear heat capacity, (iii) discovery of a scissors-like vibration mode and determination of the nature of its electromagnetic decay, (iv) discovery of enhanced low-energy γ -emission in light nuclei, and (v) measurements of vibrations of the nucleus' neutron skin. These discoveries are essential for astrophysical applications, and in particular for the understanding of the distribution of elements in our solar system. The results are also important for transmutation of radioactive waste, such that its lifetime can be dramatically reduced.

The experimental studies are based on in-beam coincidences between γ -rays and charged reaction ejectiles. The set-up includes an array of $28\ 5'' \times 5''$ NaI γ -ray detectors (CACTUS) with a total efficiency of 15 %, and a set of silicon particle telescopes. Using standard $\Delta E - E$ silicon detectors, only eight particle-telescopes could be fitted around the target inside the CACTUS target chamber because of space constraints. Therefore, the active detector area and, consequently, the detection efficiency were small, calling for a replacement by modern user-designed detectors whose properties will be described in the following.

We foresee that the new silicon ring (SiRi) will lead to more discoveries as fine structures in the data such as spin dependencies can be studied. We give a short outline of the design

requirements in section II, and in section III the silicon chip processes are described. The signal handling and acquisition system are discussed in section IV. Finally, test results and conclusions are presented in sections V and VI, respectively.

II. DESIGN PARAMETERS

The goal of the new particle-telescope system is to obtain a compact set-up with high particle- γ coincidence efficiency. Compared to the previous detector set-up with conventional silicon detectors, the goal was to obtain ten times higher efficiency without degrading the particle energy resolution or the timing properties.

The detector telescopes are designed for the measurement of energy, time, and to discriminate between different charged ejectiles from light transfer or scattering reactions. Typically, such nuclear reactions are (p,p'), (p,d) and ($^3\text{He},\alpha$), but also two-nucleon transfer reactions like (p, α) [4] and (p,t) [7]. Beam energies used are between 15 and 45 MeV. The Oslo method requires that the reaction includes exactly one outgoing charged particle. Our main interest is to measure the direct reaction product, usually in forward direction. Therefore, to avoid particle pile-up events within one and the same detector, special attention has to be given to the high elastic cross section at low scattering angles

The input basis for the Oslo method is a set of γ -ray spectra for all excitation energy bins E_x between the ground state up to the neutron separation energy S_n . However, in order to determine E_x accurately enough ($\Delta E_x < 200\ \text{keV}$), it is not sufficient to know the beam energy, reaction Q -value, and the energy of the outgoing particle. The recoil energy of the daughter nucleus also depends on the scattering angle θ between beam axis and ejectile, and thus, is directly connected to the determination of E_x . The recoil correction is of particular importance for lighter nuclei and makes it necessary to measure θ with an uncertainty of typically less than $\pm 1^\circ$.

Pile-up events and accurate excitation energy measurements require a certain granularity of the detectors. However, to avoid possible misalignments and bad overlap between the respective ΔE and E pads, and at the same time to keep the costs at a reasonable level, only the ΔE detectors were seg-

*Email address: magne.guttormsen@fys.uio.no

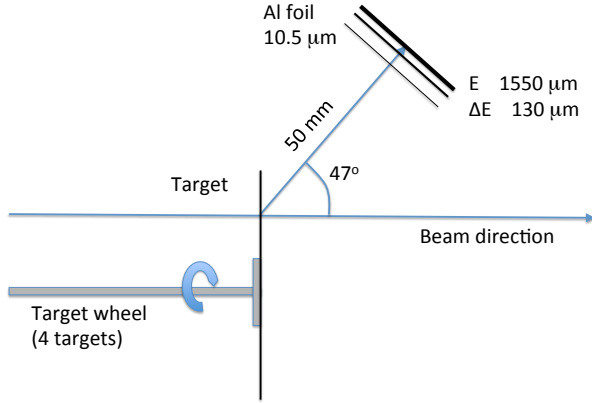


FIG. 1: Illustration of the set-up. Only one $\Delta E - E$ detector module is shown with a center at $\theta = 47^\circ$ with respect to the beam axis. One cone of aluminum foil is placed in front of all the 8 telescope modules to reduce δ -electrons impinging on the front detector. The target chamber also houses a target wheel with place for 4 targets.

mented. By requiring that only one ΔE pad fires, pile-up events in the E detector shared by the pads can be rejected.

The particle-telescopes are to be placed inside the existing vacuum target chamber of the CACTUS NaI array. The 28 NaI detectors are placed at a distance of 22 cm from the target and are distributed on a spherical frame. Each NaI is equipped with a conical 10 cm thick lead collimator between the target and detector with an opening of $\varnothing = 70$ mm at the NaI-detector front surface. The chamber is a cylindrical tube with an inner length of 48.0 cm and a diameter of 11.7 cm. To obtain reasonable high direct reaction cross sections with low spin transfer, we measure the outgoing particles at angles $\theta = 47^\circ \pm 7^\circ$ with respect to the beam axis. Lower scattering angles would give significant pile-up due to the strongly increasing elastic cross section and, thus, impose the necessity to run with lower beam current.

The center of each detector module is placed at 5.0 cm from the target. Present technology requires that the silicon wafers are flat, and we find that eight trapezoidal-shaped telescope modules form an approximate ring around target. The ΔE detectors is segmented into eight curved pads, covering mean scattering angles θ between 40 and 54° in 2° steps per pad (corresponding to ≈ 1.7 mm). Figure 1 shows the arrangement of the telescope system within the target chamber.

The detector system is designed for measuring various outgoing charged particles appearing for the projectile types and energies available at OCL. The yield of making good 2–4 cm² area detectors with thickness > 2 mm, is low due to bad bulk properties as a result of an increasing number of impurities. Also, high depletion voltages require that broad guard rings surround the active areas. A good compromise for the beam energies needed for the Oslo method, is a ΔE and E detector with thicknesses of 130 and 1550 μm , respectively. Such a telescope system will be able to measure and identify protons and ^4He -ions in the energy regions of 3.7 – 16.5 MeV

TABLE I: Particle energies deposited in the telescope. The second column gives the maximum energy deposited in the ΔE front detector, which represents the lowest energy applicable. The three columns to the right represent the highest energy that is stopped by the $\Delta E + E$ detector, and the corresponding energy deposits in the ΔE (130 μm) and E (1550 μm) detectors.

Particle type	ΔE (MeV)	$\Delta E + E$ (MeV)	ΔE (MeV)	E (MeV)
p	3.7	16.5	0.7	15.8
d	4.9	22.3	1.0	21.3
t	5.7	26.5	1.2	25.3
^3He	13.4	58.3	2.6	55.7
α	15.0	65.9	2.9	63.0

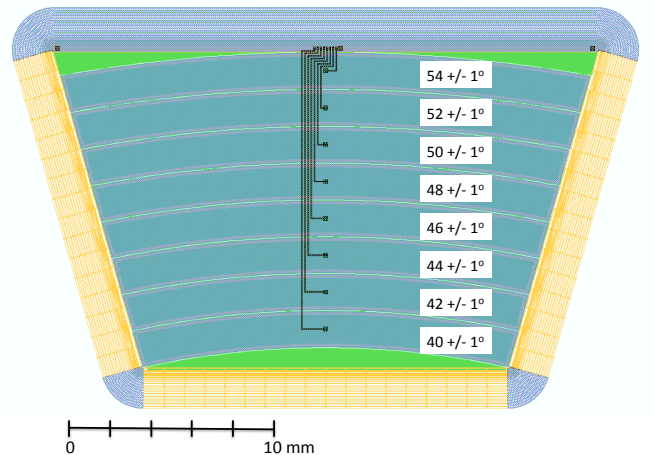


FIG. 2: Layout of the front ΔE detector. The curved pads are designed to specific angles θ .

and 15.0 – 63.0 MeV, respectively. A more complete list of particle types and energies is shown in Table I.

III. DETECTOR LAYOUT

The thick E detector (1550 μm) needs a high bias voltage in order to be fully depleted. Therefore, 18 guard rings are surrounding each detector's active area, covering a ring width of 1700 μm , which is comparable with the detector thickness. As ΔE and E detectors are mounted just behind each other, a larger active area in the thin detectors would not increase the efficiency of coincident $\Delta E - E$ measurements. In order to avoid extra mask costs, it was therefore decided to equip the ΔE detectors with the same guard-ring structure.

Figure 2 shows the layout of the thin ΔE front detector. The detector is equipped with eight curved pads so that the scattering angle θ is constant for each pad. Due to this curvature and the trapezoidal shape of the detector, an area about as large as half a pad is not used for detection, see Fig. 2. The area of the pads increases with θ . In the spherical limit (ignoring the guard rings), the corresponding solid angle covered by each

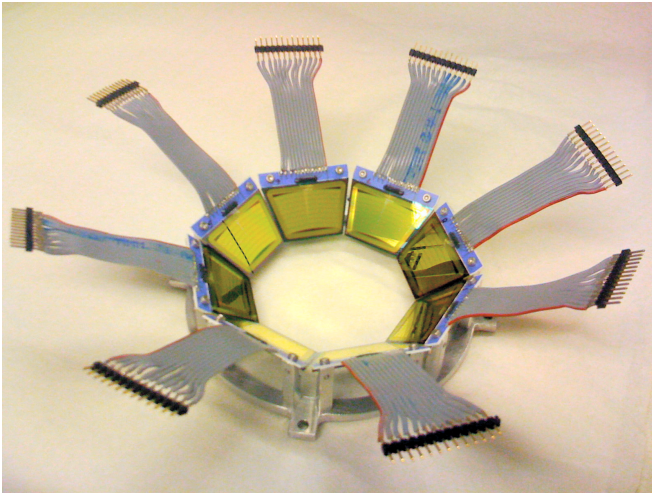


FIG. 3: Silicon particle telescope modules with connectors, mounted on the support structure centering the detectors in the reaction chamber.

pad is

$$\Delta\Omega = 2\pi \sin\theta\Delta\theta. \quad (1)$$

Thus, the solid angle covered by the 40° pad is about 21% smaller than for the 54° pad. The back E detector has the same layout as shown in Fig. 2, but is not segmented into several pads.

The ΔE and E detector chips were designed and produced by SINTEF MiNaLab, Norway. Float zone (FZ) silicon originating from Topsil, Denmark, was used in the production. The wafers for the $1550\mu\text{m}$ thick E detector were supplied directly by Topsil, while the $130\mu\text{m}$ thick wafers for the ΔE detector were procured from Virginia Semiconductor, USA, who made the wafers from a FZ Topsil ingot.

The processing sequence includes field oxidation, boron implantation for the detector readout pads and guard ring, opening of contact holes, and front and backside metalization (aluminum). As the detector readout pads are covered by aluminum, the design of the ΔE chip with eight pads requires a second layer of aluminum. This is necessary for crossing the lines connecting to the respective bonding pads over the other readout pads. The two metal layers are separated and isolated by $5\mu\text{m}$ of polyimide, and five mask layers are therefore needed for the processing (active pad and guard ring, contact holes, metal 1, polyimide, and metal 2). As the E detector chip only includes one readout pad, no second metal is needed, and the processing requires three mask layers only.

The detector full depletion voltage is inversely proportional to the specific resistivity, but increases with the square of the thickness. The thick wafers used for production of the E detector had a specific resistivity in the range $10 - 30\text{k}\Omega\text{cm}$. The detectors are to be operated fully depleted, and the typical depletion voltage was measured to $< 300\text{V}$. Another challenge is that the bulk leakage current increases with the depletion width and thereby the thickness. However, SINTEF has developed very efficient gettering processes which eliminates most

TABLE II: Silicon chip properties.

Detector type	ΔE	E
Chip #	21	23/5
Thickness (mm)	0.13	1.55
Number of pads	8	1
Pad area (mm^2)	299	323
Individual pads (mm^2)	31.5 - 43.7	-
Depletion (V)	15	220
Pad leakage (nA)	0.4 @ 30V	6.5 @ 480V
Guard leakage (nA)	0.9 @ 30V	7.3 @ 480V

of the bulk recombination centers, and typical pad and guard ring leakage currents at 480V were $< 5\text{nA}$ and $< 10\text{nA}$, respectively. Concerning the ΔE detector, the main problem was the fragility with resulting wafer breakage due to the very thin material and especially insufficient edge rounding.

Table II shows typical depletion voltages and leakage currents for the detectors.

The bonding and mounting on ceramic substrate were performed by Microcomponent, Horten. The two ΔE and E chips are glued back-to-back on the 0.5mm thick substrate. To assure redundancy, two bonding threads were used for each contact to the ceramic board. A flat cable is soldered to the board to connect to the preamplifiers. The assembled SiRi $\Delta E - E$ ring with 8 modules is shown in Fig. 3.

IV. ELECTRONICS AND DATA ACQUISITION

The telescope module of Fig. 3 is connected by multi-pole shielded cables, manufactured by Mesytec, with LEMO vacuum feedthroughs. Outside the vacuum chamber, the detectors signals are connected to preamplifiers. There are four preamplifiers for the ΔE detectors, each handling 16 pads, and one preamplifier for all eight E detectors. Both preamplifier types are Mesytec MPR-16 with sensitivities adapted to the expected energy deposits in the front and back detectors, respectively.

The preamplified signals are transferred as differential signals to Mesytec STM-16 modules including both spectroscopy amplifiers and timing-filter amplifiers, and also leading-edge discriminators. The logic OR of all E detector discriminator outputs is used to generate the trigger signal for the data acquisition.

The γ -rays detected by CACTUS are filtered off-line to select only those rays in coincidence with the respective reaction of interest. This is achieved by measuring the time difference between particle detection in the E detector (start signal) and the γ -ray detection in CACTUS (stop signal). The acquisition trigger signal is given by the logic OR of all E detector discriminator outputs, optionally AND-ed with the logic OR of all ΔE detector discriminator outputs. The stop signal is individual for each γ -ray detector, i.e., for 28 NaI and up to 2 Ge detectors.

Since we use leading-edge and not constant-fraction dis-

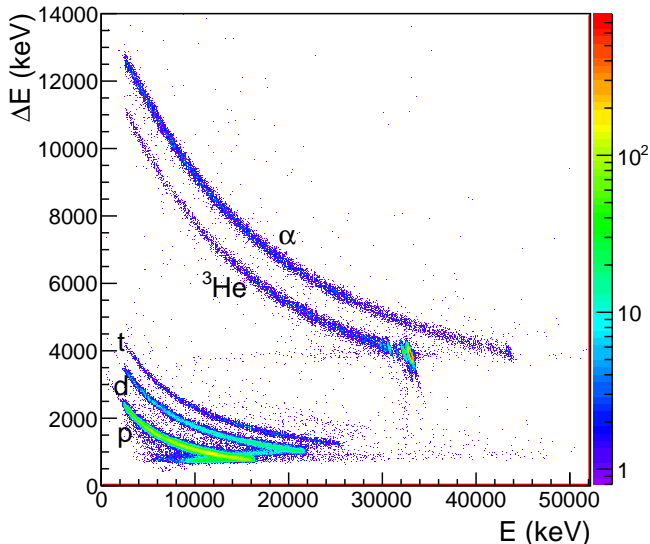


FIG. 4: $\Delta E - E$ matrix for the reaction of 38 MeV ^3He ions on a ^{112}Cd target. For this example, we have chosen front detector f5 ($\theta = 50^\circ$) and back detector b1. There are totally 64 matrices with f0, f1, ..., f7 and b0, b1, ..., b7.

criminators, the walk due to different signal rise times for different energy deposits has to be corrected in software. For this purpose, we found that a good choice for the energy-corrected time was given by

$$t(E) = t_0 + \frac{\alpha}{E + \beta} + \gamma E, \quad (2)$$

where t_0 is the measured time and α , β and γ are fitted values to ensure that $t(E)$ is approximately constant.

The data acquisition system is based on one VME crate housing commercial and custom-made VME modules. The system is controlled by software running on a CES 8062 CPU. The trigger handling is performed by a custom VME module which is capable of separating 8 different trigger sources. The analog-to-digital conversion is done using ADCs from CAEN (mod. 785) and Mesytec (MADC-32), and TDCs from CAEN (mod. 775). The data is transferred to a standard Linux PC through a CAEN VME USB module. The whole system has been run without problems at trigger rates of up to 10 kHz.

The slow-control settings of most Mesytec modules are operated via Mesytec's proprietary remote control bus using a control software developed at OCL. This remote control is very convenient for modules placed at the target station (ramping of HV and leakage current monitoring, no radiation exposure), as well as for the shaper modules (thresholds and gains, large number of channels to adjust). The thresholds and control registers of the ADCs and TDCs are set directly by the data acquisition program running on the VME CPU.

V. SYSTEM PERFORMANCE

The new SiRi particle-telescope system has already been used in several experiments at OCL. In principle there is no need for constructing a fast coincidence overlap between the ΔE and E detectors. If one back E -trapeze has triggered, also the front detector should have been hit by the same charged particle, unless the particle passed through the areas not covered by the strips. By requiring that one and only one pad of the front detector has provided a reasonably high signals, the $\Delta E - E$ particle event is assumed to be good.

Figure 4 shows a typical $\Delta E - E$ matrix for 38 MeV ^3He ions impinging on a ^{112}Cd target. The curves for each particle type are well separated, and the coincident γ rays can be assigned to a specific nucleus at a given excitation energy E_x , with $E_x < B_n$. The most energetic protons, deuterons, and tritons are not stopped in the E detector, resulting in a backbend of the respective curves.

A computer code jkinz [5] has been developed to calculate reaction kinematics and to estimate the energy losses of the various particle types in the target and other materials. The energy loss functions by Ziegler [6] are used for this purpose. The nuclear masses necessary for the relativistic treatment of the reaction kinematics are obtained from the AME2003 tables [9]. The calculation displayed in Fig. 5 demonstrates the very good resemblance with the experimental curves of Fig. 4.

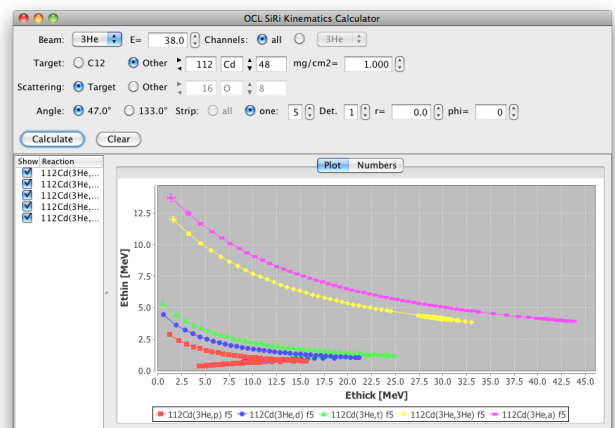


FIG. 5: Graphical user interface (GUI) of the jkinz application with parameters appropriate for the ^{112}Cd experiment of Fig. 4.

Projections of the ^3He curve of Fig. 4 on the ΔE and E axis are shown in Fig. 6. The spectra are displayed for energies around the elastic peak. The spectrum created event-by-event by adding the two detector signals $E_{\text{tot}} = \Delta E + E$ gives a resolution which is about two times better than for the E projection. The reason is that the more energy deposited in the ΔE detector, due to statistical straggling, the less energy is deposited in the E detector, and opposite. The FWHM of the elastic scattering peak in the E_{tot} spectrum is approximately 200 keV, which is very good with respect to all contributing

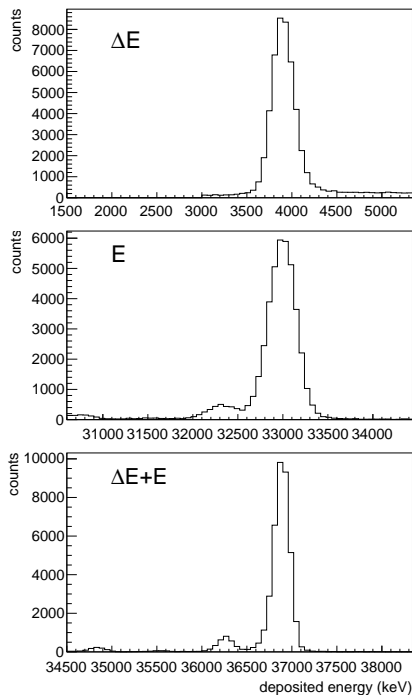


FIG. 6: Spectra of the measured $^{112}\text{Cd}(^3\text{He},^3\text{He})^{112}\text{Cd}$ elastic peak in the ΔE and E detector. The bin width is 60 keV/ch. A clear improvement in energy resolution is seen in the spectrum where ΔE and E are added event-by-event.

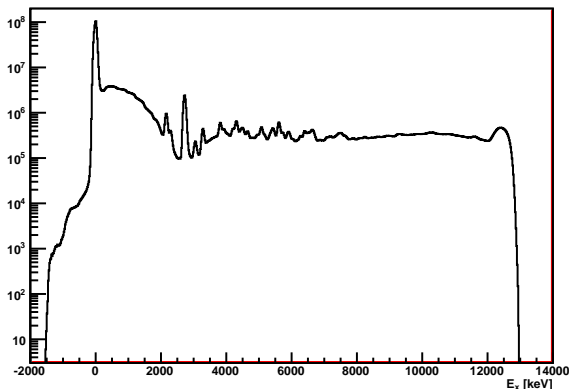


FIG. 7: Proton spectrum of the $^{90}\text{Zr}(p,p')^{90}\text{Zr}$ reaction with beam energy of 17 MeV. All 64 particle telescopes are added.

factors. The excited 2^+ state of ^{112}Cd at 618 keV is well separated from the strong elastic peak.

The main contribution to the total resolution of the E_{tot} spectra has its origin from the variation of recoil energy carried by the heavy residual nucleus; the higher scattering angle θ , the more kinetic energy is transferred to the residual nucleus. This effect can be reduced by lighter projectile with lower incident energy, and/or by using heavier targets.

Figure 7 shows the results from a typical light-ion experiment [7] with 17 MeV protons on ^{90}Zr . The experimen-

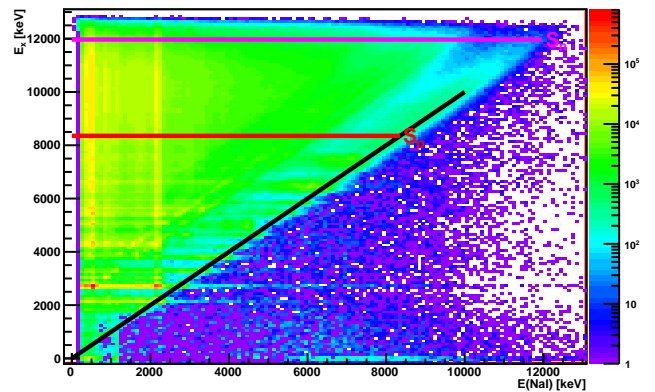


FIG. 8: Proton- γ coincidences giving the $E_x - E_\gamma$ matrix, which is the starting point for the Oslo method. It should be noted that the NaI spectra are raw, meaning they have not been unfolded by the NaI detector response function. The horizontal lines marked S_p and S_n indicate the proton and neutron binding energies, respectively.

tal resolution for the ground state in (p,p') scattering on 1.83 mg/cm^2 ^{90}Zr is now $\text{FWHM} \approx 100 \text{ keV}$, corresponding to a standard deviation of $\sigma \approx 43 \text{ keV}$. This resolution includes the straggling in the target and the uncertainty in the scattering angle determination. It also includes all misalignments of the detector system.

The elastic peak is seen to be more than 100 times stronger than the average (p,p') cross-section to excited states in ^{90}Zr . The rate of pile-up events is 4 orders of magnitude lower than the elastic peak. The particle yield at the right-hand tail of the elastic peak is due to $\approx 20\%$ punch-through of the elastic events.

A good SiRi particle event is to be taken in coincidence with the NaI and Ge detectors of the CACTUS array. Here, the 32-fold TDC gives the time difference between the E detector and the individual γ detectors. In the event sorting procedure, the energy-compensated time difference is reconstructed by

$$\Delta t(E_{\text{back}}, E_\gamma) = \Delta t_0 - t_p(E_{\text{back}}) - t_\gamma(E_\gamma), \quad (3)$$

where the two last terms are calculated from Eq. (2). The two sets of α , β and γ parameters needed, were fitted to data from a separate run on a ^{12}C target. In practice, it is usually sufficient to set each NaI detector's t_0 value such that all detectors are aligned at $E_\gamma = 4.43 \text{ MeV}$, and then use the same energy-dependent correction to all NaI detectors, as the output signal amplitudes of the NaI detectors are usually adjusted to be very similar to each other. A similar procedure is applied for the time signals of the E detectors. Here, the corrections are usually small because of the fast signals from the E detector and the high ejectile energy and small energy interval ($E_x < 8 - 12 \text{ MeV}$) of interest.

For low energy signals, α is the most important parameter describing the hyperbolic energy dependence of the trigger time close to the energy threshold. Here, we find $\alpha < 0$ for the START E_{back} detector and $\alpha > 0$ for the STOP γ detectors since the low energy signals produce delayed leading-edge

discriminator triggers. The procedure for making energy-compensated time spectra works very good and the resulting total time resolution of 8 particle telescopes and 28 NaI detectors is about $\text{FWHM} = 15 - 20\text{ns}$. The main contribution to the resolution comes from the NaI PMTs, which are optimized for good energy resolution, and not time.

Figure 8 shows the results from the particle- γ coincidence measurement. The relation between particle energy and excitation energy is established using calculations performed with the jkinz application, so that the excitation energy can be deduced from the particle energy. A prompt time gate is set on the coincidence peak of the $\Delta t(E_{\text{back}}, E_{\gamma})$ spectrum for incrementing the (E_{γ}, E_x) entries event-by-event, and a time gate on the random coincidences is set for decrementation. Also a gate on the proton particle $\Delta E - E$ curve is required to reduce the occurrence of unwanted events originating from pile-up, δ -electrons, incomplete energy deposits, channeling effects in silicon and so on.

The data of Fig. 8 fall mostly within the triangle defined by $E_{\gamma} < E_x$. The small number of counts outside this triangle shows that the coincidences are true and the pile-up is small. Some γ -ray lines are seen as vertical lines. They represent yrast transitions passed in almost all cascades for a large range of initial excitation energies, up to the neutron separation energy of $E_x = S_n \approx 12\text{MeV}$.

VI. CONCLUSION

The SiRi particle-telescope system has been used in various experiments at the Oslo Cyclotron Laboratory. The system

is able to identify the charged particle type using the well-known $\Delta E - E$ curve gating technique. The particle resolution is better and the efficiency is about 10 times higher than with the previous set-up of conventional silicon detectors.

SiRi also allows to study ejectiles in 8 angles with $\theta = 40 - 54^\circ$ relative to the beam direction, and 8 angles around the beam axis with $\phi = 0 - 360^\circ$. This gives the opportunity to explore the angular momentum transfer in the direct reactions.

The combined SiRi-CACTUS system has also been tested, giving very nice particle- γ coincidences. The random coincidences are subtracted in a satisfactory way, and the measurements are not affected by severe pile-up effects, provided that the beam current is typically less than $\approx 2\text{nA}$. By utilizing the ejectile- γ -ray angular correlations, information on the multiplicities of the γ transitions should be possible to deduce as function of initial excitation energy.

We believe that the good-resolution, high-efficiency particle- γ coincidence system will open for the study of new physics in the quasi-continuum of atomic nuclei.

Acknowledgments

Financial supports from the Norwegian Research Council (NFR) and the University of Oslo are gratefully acknowledged. We also thank A. Schiller and A. Werner for their contribution in the early stage of the project, and A.C. Larsen for preparation of Figs. 4 and 6.

-
- [1] A. Schiller, L. Bergholt, M. Guttormsen, E. Melby, J. Rekestad, and S. Siem, Nucl. Instrum. Methods Phys. Res. A **447**, 498 (2000).
 - [2] U. Agvaanluvsan, A.C. Larsen, M. Guttormsen, R. Chankova, G. Mitchell, A. Schiller, S. Siem, and A. Voinov, Phys. Rev. C **79**, 014320 (2009).
 - [3] A.C. Larsen, M. Guttormsen, R. Chankova, T. Lönnroth, S. Messelt, F. Ingebretsen, J. Rekestad, A. Schiller, S. Siem, N.U.H. Syed, and A. Voinov, Phys. Rev. C **76**, 044303 (2007).
 - [4] A. Bürger, S. Hilaire, A.C. Larsen, N.U.H. Syed, M. Guttormsen, S. Harissopoulos, M. Kmiecik, T. Konstantinopoulos, M. Krtička, A. Lagoyannis, T. Lönnroth, K. Mazurek, M. Norby, H. Nyhus, G. Perdikakis, S. Siem, and A. Spyrou, Phys. Rev. C, in preparation
 - [5] A. Bürger, OCL SiRi Kinematics Calculator, University of Oslo, 2011, <http://tid.uio.no/~abuenger/>
 - [6] J.F. Ziegler, J.P. Biersack, and U. Littmark, *The Stopping and Range of Ions in Solids*, Pergamon Press, New York (1985)
 - [7] A. Bürger, S. Siem, A. Görgen, M. Guttormsen, T.W. Hagen, A.C. Larsen, P. Mansouri, M.H. Miah, H.T. Nyhus, Th. Renstrøm, S.J. Rose, N.U.H. Syed, H.K. Toft, G.M. Tveten, A. Voinov, and K. Wikan, Phys. Rev. C, in preparation
 - [8] H.K. Toft, A.C. Larsen, A. Bürger, *et al.*, PRC, accepted (2011)
 - [9] G.Audi, A.H.Wapstra, and C.Thibault, Nucl. Phys A**729**, 337–676 (2003)